SEMARAK ILMU PUBLISHING

Journal of Advanced Research in Fluid Mechanics and Thermal Sciences

Journal homepage:
https://semarakilmu.com.my/journals/index.php/fluid_mechanics_thermal_sciences/index
ISSN: 2289-7879

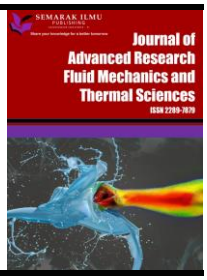

Experimental Investigation of Temperature Homogeneity and Peak Temperature in a Battery Pack of Cylindrical Li-ion Cells Under Free and Forced Convection

Manmeet Singh[1,*], Sudhanshu Dogra[1], Ravindra Jilte[1]

[1] Department of Mechanical Engineering, Lovely Professional University, Phagwara-144001, India

ARTICLE INFO

Article history:
Received 13 August 2024
Received in revised form 9 November 2024
Accepted 21 November 2024
Available online 10 December 2024

Keywords:
C-rate; battery tester; lithium iron phosphate; li-ion batteries; forced convection

ABSTRACT

Electrical vehicles (EVs) are emerging as a suitable replacement for conventional IC engine-based automobiles because of their environmental friendliness. An EV is powered by a rechargeable battery pack usually made of Lithium-ion batteries and these batteries generate heat during their operation cycle due to exothermic reactions and ohmic effect. Thermal management of batteries is important for their safe operation and optimum lifespan. In this paper, a comparative analysis of temperature homogeneity, peak temperature and average temperature of battery pack is presented between free and forced convection-based Battery Thermal Management System (BTMS). Cells that are at higher temperature than average temperature of battery pack are more liable to fail earlier as compared to other cells of pack. Present research focuses on finding such critical cells in a battery pack consisting of twelve lithium-ion batteries. The battery pack is discharged at three different rates: 1C, 2C and 3C, and temperature of each cell is measured at regular intervals during the discharge process. The experimental results from present study revealed that free convection is better at maintaining temperature homogeneity, but peak temperatures were above 50˚C. Forced convection based BTMS was able to keep peak temperatures below 50˚C at 1C discharge rate but temperature homogeneity was not maintained within ideal limits of 5˚C. At higher discharge rates, the performance of both free convection and forced convection based BTMS is not within acceptable limits. Critical cells were identified to get better insight into limitations of conventional cooling systems so that better layout of battery module and better alternative methods of battery pack cooling can be developed.

1. Introduction

In the past few years, extensive research has been conducted on Electrical vehicles (EVs) as it presents an alternative to conventional petroleum-based IC engines. EVs can reduce car emissions as electricity can be generated from clean energy sources like solar, tidal and hydro [1]. The power source of all EVs is a battery, which stores and provides energy at desired rates as per EV operating conditions. The battery pack has battery cells arranged in a certain layout: cubical, cuboid, circular,

* *Corresponding author.*
E-mail address: manmeet.jt@gmail.com

https://doi.org/10.37934/arfmts.125.1.4256

serpentine, or hexagonal etc. In terms of cost minimization, cubic layout is best but hexagonal arrangement is most efficient in space utilization [2]. Various types of rechargeable battery cells can be used to power EVs of which Lithium-ion (Li-ion) batteries are widely used. As compared to Nickel Metal Hydride battery, Nickel-Hydrogen battery and fuel battery, Li-ion batteries offer many advantages: they are compact, they have stable and better life cycle, they have high energy density and low self-discharge rate [3,4]. High energy density and higher capacity battery cells are an essential requirement of EVs as these factors directly affect driving range. Li-ion cells come in various shapes and configurations like cylindrical, pouch, prismatic etc. but cylindrical cells are more popular due to their compactness and energy density [5]. Cylinder 18650 cells are extensively used by many vehicle manufacturers to their small size and high energy density. Cells like 32650 and 21700 have about 50% more energy capacity than 18650 but they have less energy density as compared to 18650 [6]. A major challenge presented by high energy density batteries is their higher heat generation rates. Excessive heat accumulation inside battery pack can increase battery temperature to such an extent where they can swell, explode, and become hazardous to an EV user and environment. In the present study, 32650 LiFePO4 (LPF) cells are selected due to their safe nature of operation and characteristics like more popular 18650 Li-ion cells. Batteries are electrochemical cells and there is strong correlation between charge/discharge rates (C-rates) with temperature of battery [7]. A battery pack must operate under extreme cold and hot climates at high C-rates [8]. The capacity of Li-ion cells is strongly affected by temperature. A study conducted on 18650 cells showed that after 800 cycles capacity loss was 36% at 45˚C, but capacity loss increased to 70% after just 490 cycles at 55˚C [9]. Temperature uniformity or homogeneity must be ensured inside battery pack. Temperature uniformity (ΔT) means the difference between cell-to-cell temperature. A higher temperature difference creates electrochemical imbalance that causes deterioration of the whole battery pack. The temperature uniformity or homogeneity should be maintained within 5˚C in a battery pack and peak temperature should not exceed 50˚C [10,11]. Temperature above 70˚C can cause thermal run away of batteries where they generate excessive heat due to exothermic reactions. For every degree increase between 30˚C and 40˚, the Li-ion battery lifespan is reduced and batteries age prematurely [12]. At low temperature, the performance of Li-ion batteries reduces significantly. The availability of energy of 18650 cell drops to 60% at -20˚C as compared to normal ambient temperature [13]. At extreme cold temperatures of -40˚C, 18650 cell only deliver 1.25% and 5% of the initial power capacity and energy capacity [14]. Li-ion batteries perform best in the temperature range of 20°C–40°C and this range is regarded as ideal operating range [15-18]. A more relaxed threshold for modern batteries can be 50˚C [19]. Based on operating temperature, three levels of performance of batteries can be considered: optimal limit, acceptable limit, and safety limit. The optimal limit, acceptable limit, and safety limit of peak temperature (T_{max}) for a battery pack can be kept at 40˚C, 50 ˚C and 60 ˚C respectively [20]. The need for a thermal management system for batteries arises because of the issue concerning dependence of Li-ion batteries performance on temperature. A Battery Thermal Management System (BTMS) is required to maintain the temperature of battery pack within ideal limits of temperature. A good BTMS should satisfactorily work under hot and cold climates at various C-rates, consuming low power, while keeping cost and complexity to minimum [21]. There are mainly two types of BTMS: Active and Passive, as indicated Figure 1. Passive BTMS do not consume any energy while operational and they are generally based on free convection. Utilization of heat pipes and phase change materials has become an area of interest for enhancing performance of passive thermal management systems [22]. Active systems are usually based on forced convective and have components like fan, blower, or pump. Liquid cooling is nowadays the most widely used active cooling system adopted in EVs. Both active and passive systems can also be combined to form hybrid BTMS for better control of temperature uniformity and maximum temperature within battery pack.

In present research, a comparative study in terms of three important parameters: temperature uniformity, peak temperature, and average temperature of battery pack, is presented for forced convection based BTMS (BMTS-FO) and free convection based BTMS (BTMS-FR). Cells which have higher surface temperature are identified as critical cells. The variations in temperature of battery cells across battery pack may be due to air flow pattern, shape of battery cells, battery pack design and in certain cases inherent disadvantage of BTMS systems, for example: Inherent disadvantage of air and liquid cooling is rise of temperature of coolant when it flows from inlet to outlet. Maintaining temperature homogeneity and restricting peak temperature within ideal range is a challenge. Critical zone and critical cell identification inside battery pack is important for proper dissipation of heat and control of temperature [23]. By identifying critical cells, a better layout of battery pack can be designed and hybrid BTMS can be developed which can overcome limitations of liquid and air-cooling systems.

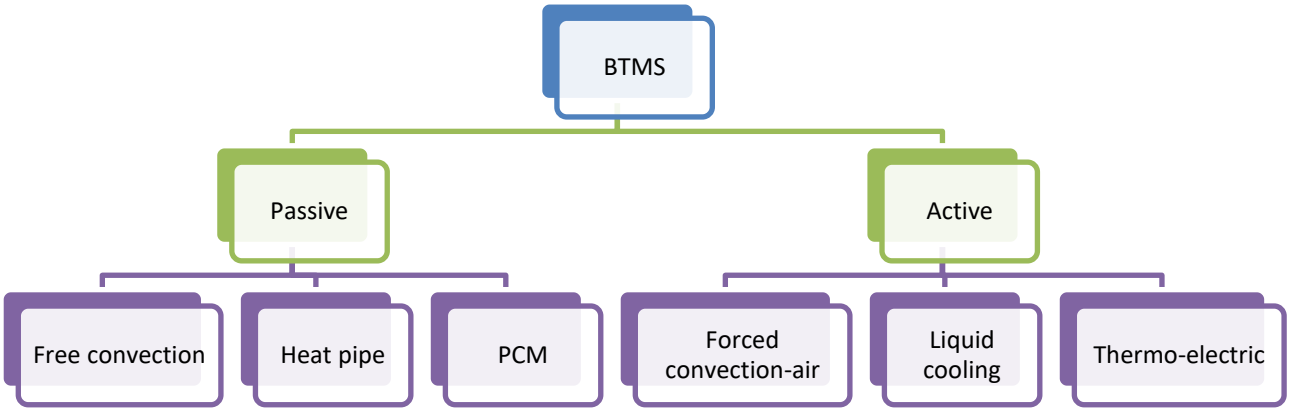

Fig. 1. Battery thermal management systems of EVs

2. Methodology and Experimentation

2.1 Development of Experimental Facility

EVs power source is batteries connected in series or parallel arrangement inside a battery pack. The present work experimentation facility consists of a battery pack, a battery tester with LAN connection to computer, a 16-channel data logger and K- type thermocouples, a power supply, an acrylic casing, and a variable speed cooling fan. In present work, the battery pack consists of twelve Lithium Iron Phosphate (LFP) cylindrical battery cells connected in series connection. Selected cells are popularly known as 32650 LFP cells as their diameter is 32 mm and height are 65 mm. Specification of LFP cells as provided by manufacturer is given in Table 1. Cells are arranged in 3×4 layout and total length (L) and width (W) of battery pack is 100 mm and 134 mm, respectively. The interspacing between battery cells was kept at 2 mm. The schematic of test facility, dimension of battery pack as well as battery cell, can be seen in Figure 2. The experimental facility development is based on our earlier research work as shown in Figure 3 [24]. The Temperature homogeneity (ΔT) across battery pack is measured by fixing K-type thermocouples with probes designed to match the surface of cylindrical cells. Inlet air temperature (T_i) and outlet air temperature (T_e) in case of BTMS-FO and, ambient temperature (T_∞) in BTMS-FR is measured by K-type thermocouples with cylindrical probes. Thermocouples are connected to a 16-channel data logger which stores data after fixed intervals of time as per requirement. The data logger is connected to the computer to extract the data. The battery tester discharges and charges battery pack at desired C- rates by controlling current and voltage. The charge mode of battery is constant current and constant voltage while discharge mode is constant current. The battery tester voltage and current can be varied with steps of 0.1 V

and 0.1 Ampere, respectively. The charging and discharge voltage can be varied between 9 V to 99 V with maximum power available as 900 W. The battery tester communication port is connected through LAN connection to computer. A cooling fan is installed at the inlet section in case of forced convection (BTMS-FO). The diameter of the cooling fan is 105 mm and mass flow rates are calculated by taking average air velocity as mentioned in section 2.2.

Table 1
Battery cell (LFP) specifications

LPF battery cell nominal voltage	3.2 V
Capacity of each cell	6 Ah
Maximum depth of discharge	70%
Cut-off voltage to kept in discharging	2 V
Maximum discharging rate	3C
Cut-off voltage in charging	3.7 V

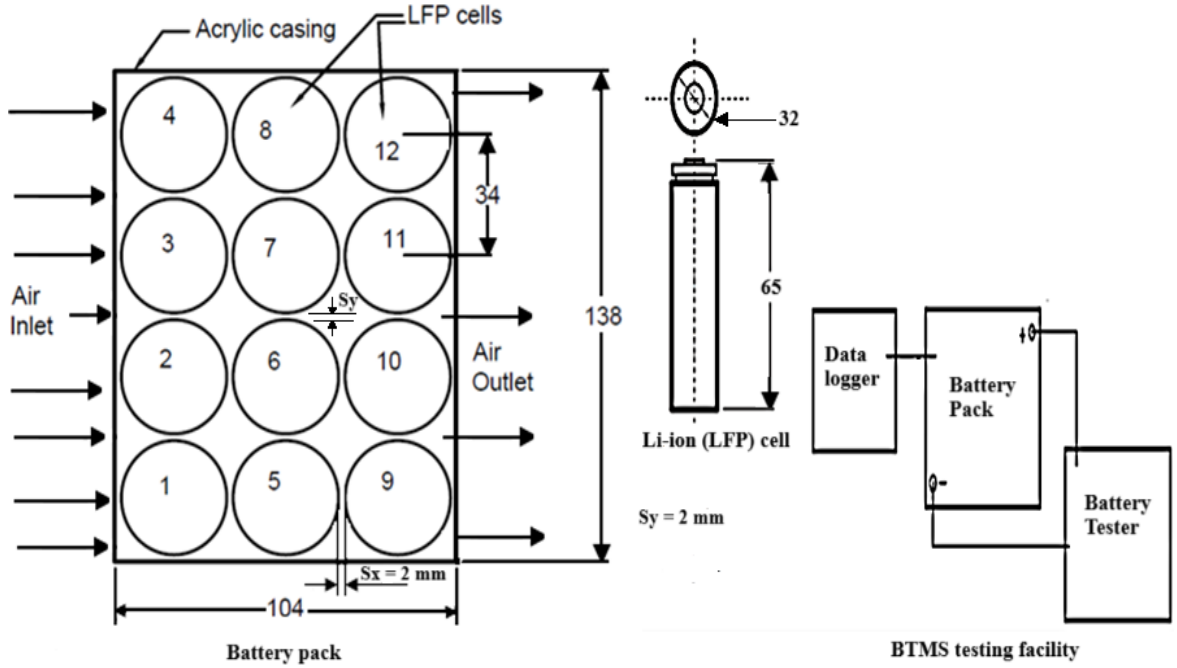

Fig. 2. Battery pack, Battery cell (LFP) and BTMS testing facility

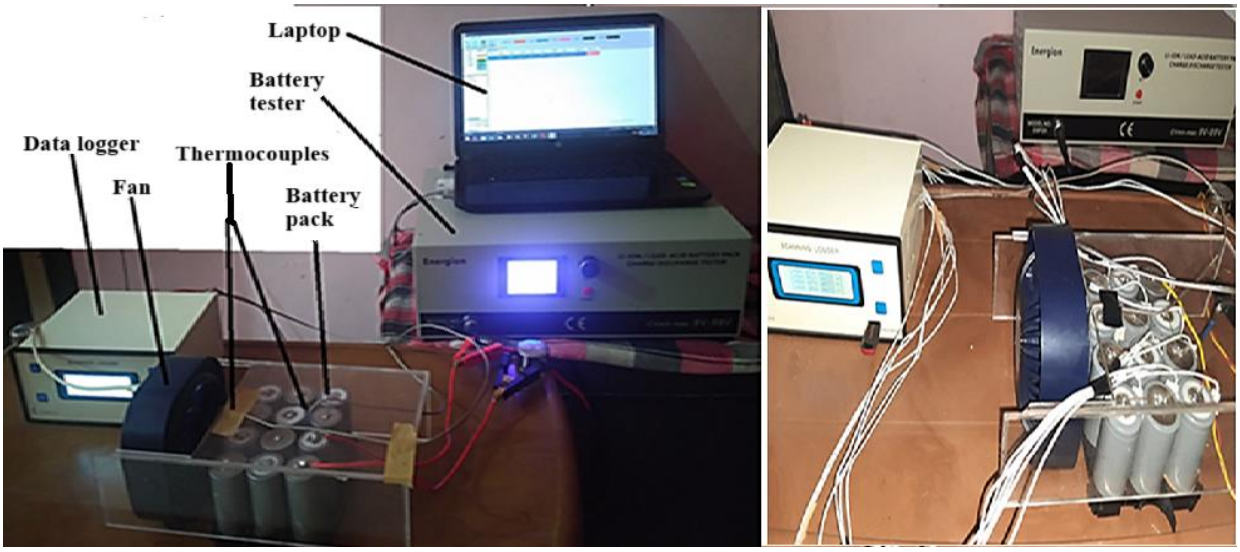

Fig. 3. Experimental facility [24]

2.2 Experimental Procedure

The experimental study was conducted at three discharge rates: 1C, 2C and 3C. The cut-off voltage and maximum voltage of battery pack were kept at 22 V and 42 V, respectively. A comparative study was conducted to check experimental results against correlations available for forced convection. BTMS-FR and BTMS-FO were compared based on three important parameters:

i. Average temperature (T_{avg}) of battery pack.
ii. Peak surface temperature (T_{max}) of battery cells.
iii. Temperature homogeneity (ΔT) inside battery pack.

The air inlet velocity in the case of BTMS-FO was measured by an anemometer. As the air velocity varies across cross-section of fan, average inlet air velocity (V_{avg}) was calculated by taking measurements at four separate locations (1, 2, 3 and 4) as shown in Figure 4. The temperature readings were periodically taken by thermocouples and the battery pack average temperature (T_{avg}), peak surface temperature (T_{max}) of cells and temperature homogeneity (ΔT) were calculated as given by Eq. (8), Eq. (9), and Eq. (10).

The experimental results were compared with available empirical correlations related to forced and free convection. Initial measurements done before the start of experiment and other important parameters are listed in Table 2.

Table 2
Parameters related to experimentation

Parameters	Value
Initial Voltage of battery pack (V_i)	38.65 V to 40.10 V
Ambient (Inlet) temperature of air (T_i)	30˚C
Average value of air inlet velocity	$V1_{avg}$ = 3.6 m/sec, $V2_{avg}$ = 4.6 m/sec, $V3_{avg}$ = 5.5 m/sec
Area of cooling fan (A_f)	8655 mm^2
Velocity at the inter-spacing	V1 = 61.2 m/sec, V2 = 78.2 m/sec, V3 = 93.5 m/sec
Transverse distance between cells (S_T), ($S_T = D + S_y$)	34 mm
Rate of discharge	1C, 2C and 3C

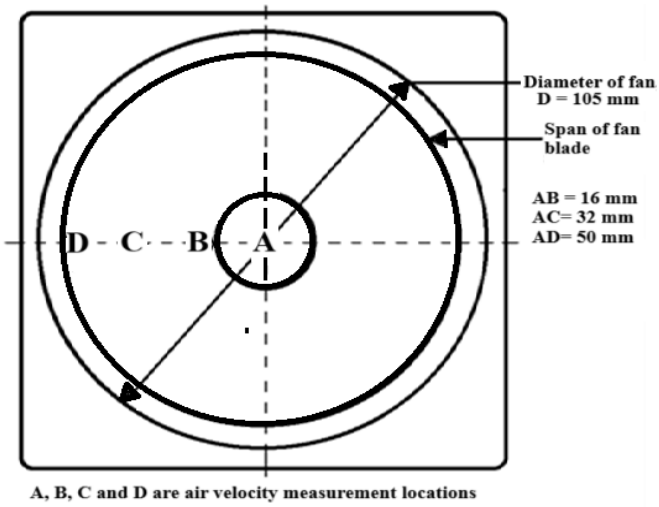

Fig. 4. Anemometer velocity measurement locations on fan cross-section

The results in forced convection were calculated by considering case of in-line arrangement where air is flowing across the bank of tubes. Reynolds number (Re_D) is calculated based on air velocity at minimum cross-section area (V1, V2 and V3) i.e., where the interspacing between cells is minimum. The value of V1, V2 and V3 and Re_D are calculated as given by Eq. (1) and Eq. (2).

$$V1 = \frac{(S_T)}{(S_T - D)} V_{1-avg} \, , V2 = \frac{(S_T)}{(S_T - D)} V_{2-avg} \, , V3 = \frac{(S_T)}{(S_T - D)} V_{3-avg} \tag{1}$$

$$Re_D = \frac{\rho_f V_{max} D}{\mu_f} \tag{2}$$

Where density of air is ρ_f, diameter of cells is D (32 mm), transverse distance between cells is S_T and dynamic viscosity of air is μ_f. All properties of air were taken at arithmetic mean temperature (T_m) of fluid, $(T_i + T_e)/2$, where T_i and T_e are inlet and outlet temperature of air, respectively. The correlation proposed by Žukauskas [25] for bank of tubes (in-line arrangement) was used for Nusselt number calculation (Eq. (3)).

$$Nu_D = C \, (Re_D)^m \, Pr^n \left(\frac{Pr}{Ps}\right)^{0.25} \tag{3}$$

The values of C, m and n at Reynolds number calculated are 0.27, 0.63 and 0.36, respectively. All properties except Prandtl number P_S were determined at arithmetic mean temperature of air (T_m). As proposed by Žukauskas [25], a correction factor of 0.86 is applied to Nu_D as number rows are three.

$$Nu_{D,corrected} = 0.86 \, Nu_D = 0.86 \frac{hD}{k_f} \tag{4}$$

Where thermal conductivity of air is k_f, heat transfer coefficient is h and diameter of cells is D. Heat transfer rate is determined using Newton's law of cooling in case of correlations results and energy balance approach for battery pack.

$$Q = NhA_s(\Delta T_{lm}) = \, m_f c_p (T_e - T_i) \tag{5}$$

Where N is total number of cells, is curved surface area of each cell is A_s, mass flow rate of air is m_f and specific heat of air is c_p. Logarithmic mean temperature difference (ΔT_{lm}) is determined by Eq. (6).

$$\Delta T_{lm} = \frac{(T_{avg} - T_e) - (T_{avg} - T_i)}{\ln[(T_{avg} - T_e)/(T_{avg} - T_i)]} \tag{6}$$

Where the average surface temperature of cells is T_{avg}. The experimental results are very well in agreement with correlation results as shown in Figure 5.

In case of free convection, the values of heat transfer coefficients (h) are calculated based on Nusselt number (Nu) obtained from the relations suggested by Churchill and Chu [26] over entire range of Rayleigh number (Ra_L).

$$Nu = \frac{hL_c}{k} = \left\{0.825 + \frac{0.387 \, Ra_L{}^{1/6}}{[1 + (0.492/Pr)^{\frac{9}{16}}]^{8/27}}\right\} \tag{7}$$

where Ra_L is Rayleigh number, Pr is Prandtl number, k is Thermal conductivity and L_c is Characteristic length (i.e., height of cell). For calculation purpose, height of cell is taken as 63 mm as 2 mm remain inside spacer and that part is not exposed to ambient air. All properties of air are evaluated at Film Temperature (T_f), $T_f = \frac{T_\infty + T_s}{2}$, where ambient temperature of air is T_∞ and average surface temperature of battery pack is T_s. The calculated values of heat transfer coefficient are well within the establish range of heat transfer coefficient for free convection as available in previous study by Kosky *et al.,* [27] as shown in Figure 6.

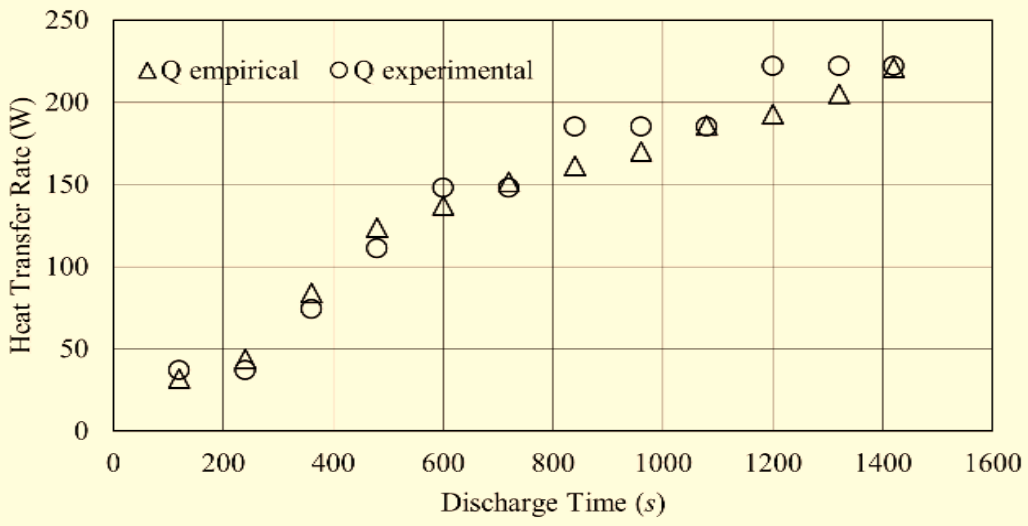

Fig. 5. Empirical and Experimental results under forced convection at 2C discharge rate

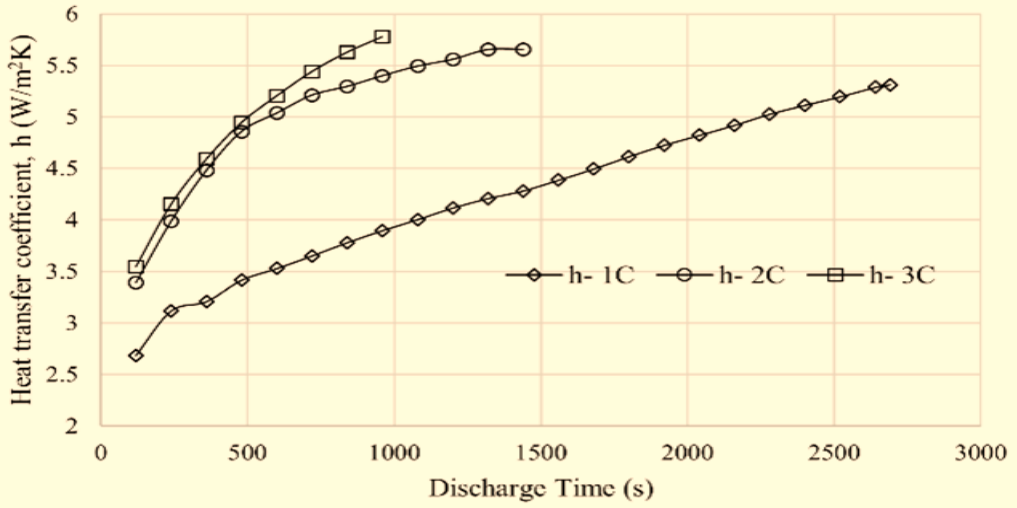

Fig. 6. Heat transfer coefficient under free convection at 1C, 2C and 3C discharge rates

3. Results

Experimental evaluations were conducted in free and forced convection based BTMS at three discharge rates: 1C, 2C and 3C. Before starting experiment, cells were assessed for voltage with the help of digital multi-meter, and it was about 3.2 V for each cell with only 5% variation from nominal voltage allowed. Typical discharge curves for 1C, 2C and 3C discharge rates, can be seen in Figure 7.

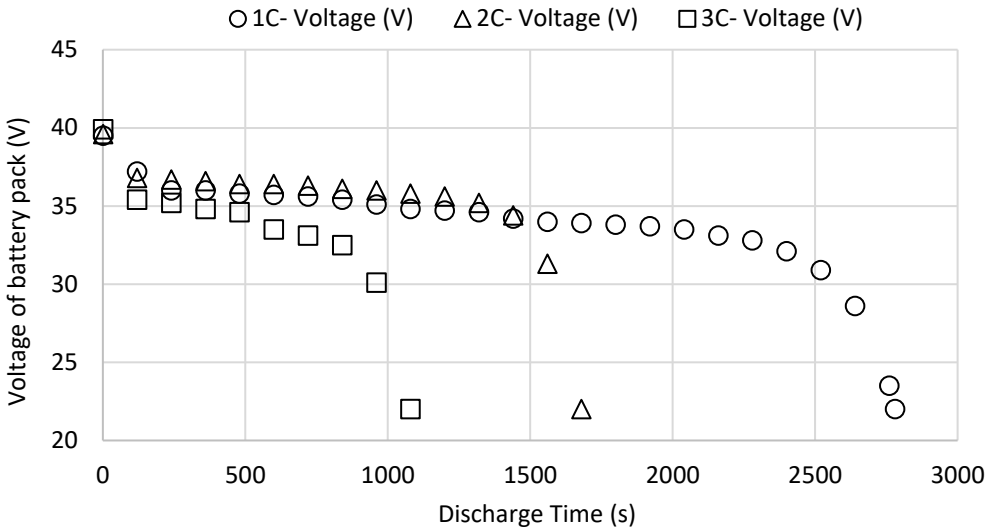

Fig. 7. Typical discharge curves at 1C, 2C and 3C discharge rates

3.1 Average Temperature of Battery Pack Under Free and Forced Convection

The temperature of all twelve cells were measured under discharge conditions of 1C, 2C and 3C and average temperature (T_{avg}) inside battery pack during was calculated as:

$$T_{avg} = \frac{\sum \text{Cell temperature}_{1,2,3,4,5,6,7,8,9,10,11,12}}{\text{Number of cells}} \tag{8}$$

Average temperature of battery pack under discharge rates of 1C, 2C and 3C, can be seen in Figure 8 resp. The discharge process is completed when cut-off voltage of 22 V is reached for battery pack. The battery pack took least time to reach cut-off voltage at 3C discharge rate, but still in both free and forced convection, the average temperature of battery pack was highest at 3C rate of discharge. Beside discharge rate, the average temperature is also affected by air inlet velocity with higher values at lower inlet velocities at same discharge rate. Average temperature variations due to layout of battery pack was evaluated by calculating average temperature of each row of battery pack (Eq. (9)). The results showed that mid row consisting of cells 5, 6, 7 and 8 has higher average temperature in free convection whereas the last row consisting of cells 9, 10, 11 and 12 has higher average temperature in forced convection.

$$\begin{aligned} T_{avg-row1} &= \frac{\sum \text{Cell temperature}_{1,2,3,4}}{4}, \\ T_{avg-row2} &= \frac{\sum \text{Cell temperature}_{5,6,7,8}}{4}, \\ T_{avg-row3} &= \frac{\sum \text{Cell temperature}_{,9,10,11,12}}{4} \end{aligned} \tag{9}$$

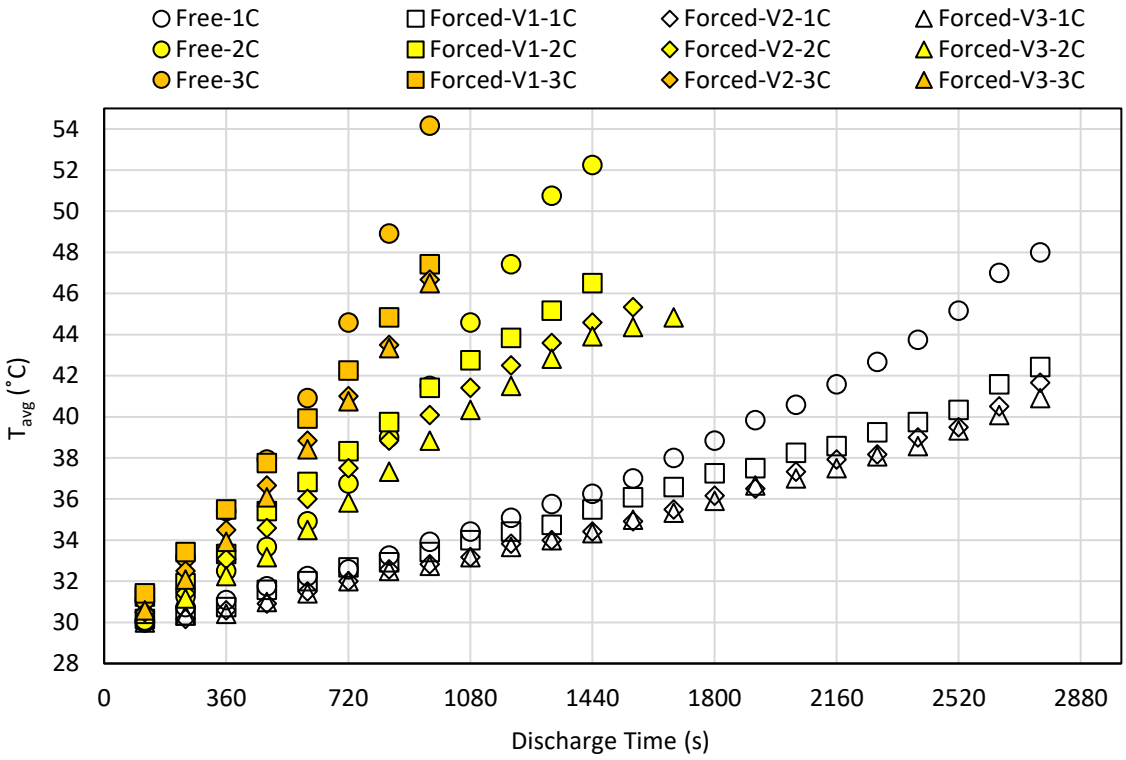

Fig. 8. Average temperature of battery pack under various combinations inlet air velocity and discharge rate for free and forced convection

3.2 Peak Temperature Inside Battery Pack Under Free and Forced Convection

The values of maximum or peak temperature (T_{max}) measured inside battery pack at various combinations of discharge rates and air velocities are shown in Figure 9 and Figure 10. A battery pack performs efficiently when operated within threshold limits of peak temperature [8]. Three threshold limits of peak temperature are:

i. Ideal or optimal limit – T < 40˚C
ii. Acceptable limit – T < 50˚C
iii. Safety limit – T < 60 ˚C

As can be seen in Figure 10, free convection based BTMS-FR is not able to maintain peak temperature within ideal limit and acceptable limits, although safety limit is maintained under free convection. Forced convection based BTMS-FO successfully maintain peak temperature within acceptable limit at lower discharge rates, and at higher air inlet velocities. Higher peak temperatures have been seen at 3C discharge rate at V1 air inlet velocity for forced convection due to increased heat generation as compared to 2C and 1C rates. Identification of critical cells is important as these cells may fail earlier due to higher stress as compared to other cells of battery pack. The cells 6 and 7 and cells 9, 10, 11 and 12 respectively are identified as critical in free and forced convection. The surface temperature of identified critical cells is higher as compared other cells of battery pack during discharge process (Figure 9). To counter the problem of uneven cooling in free and forced convection, and in forced convection alternative methods needs to be explored.

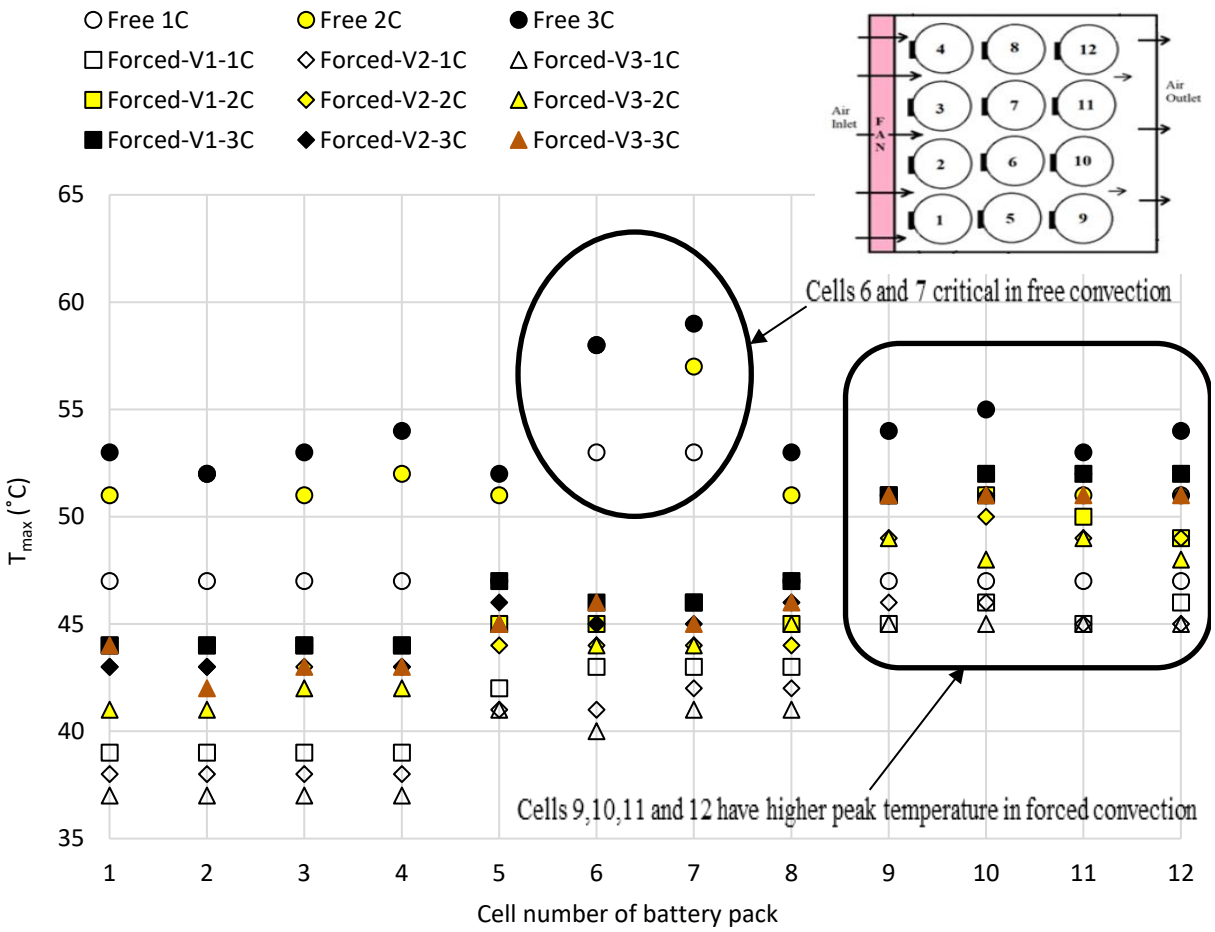

Fig. 9. The peak temperature of each cell at various combinations of discharge rate and air inlet velocity under free and forced convection

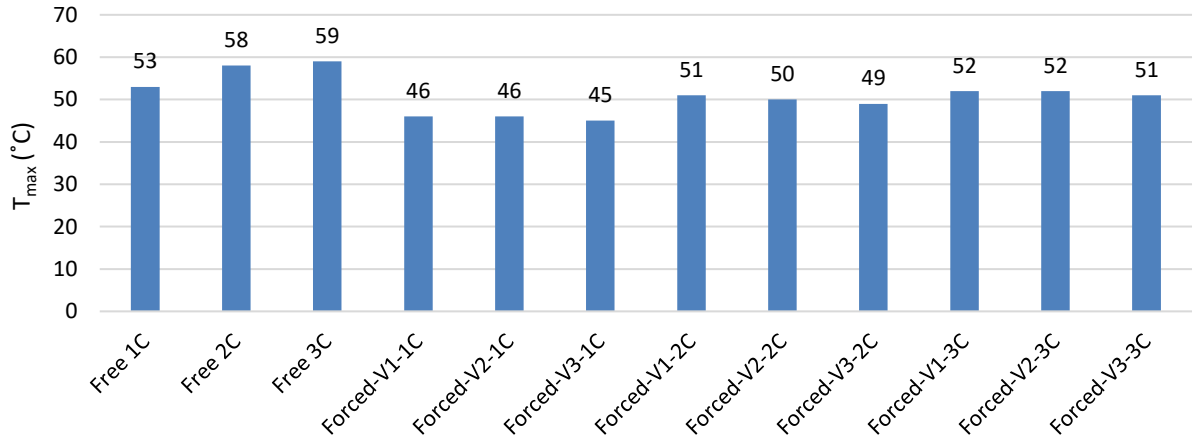

Fig. 10. Peak temperature in battery pack under free and forced convection at various combinations of discharge rates and air inlet velocity

3.3 Temperature Homogeneity of Battery Pack Under Free and Forced Convection

The maximum value of temperature non-uniformity (non-homogeneity) (ΔT_{max}) at end of discharge process is shown in Figure 11. The temperature variations inside battery pack at cell level during entire discharge process is measured at time intervals of 2 minutes (Eq. (10)).

$$\Delta T = (T_{max} - T_{min})_{\text{at time of discharge=t seconds}} \quad (10)$$

A BTMS should ideally maintain temperature homogeneity below 5˚C, and acceptable limit decided in present work is 7˚C. As seen in Figure 11 and Figure 12, temperature homogeneity at 1C-rate is much better as compared to 2C and 3C discharge rates. Increase in air inlet velocity has adverse effect on temperature uniformity and at higher discharge rates for forced convection (BTMS-FO), it exceeded the value of acceptable limit. Maximum value of ΔT for battery pack during discharge process are given in Figure 12. Results showed that the performance of free convection is better as compared to forced convection in maintaining temperature homogeneity.

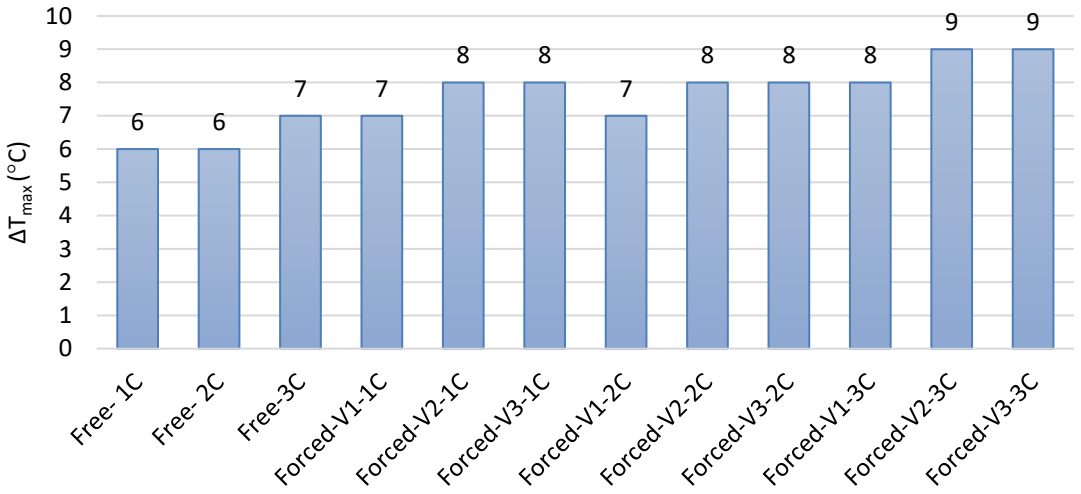

Fig. 11. Temperature homogeneity maximum values during discharge process for free and forced convection based BTMS at various discharge rates and air inlet velocity

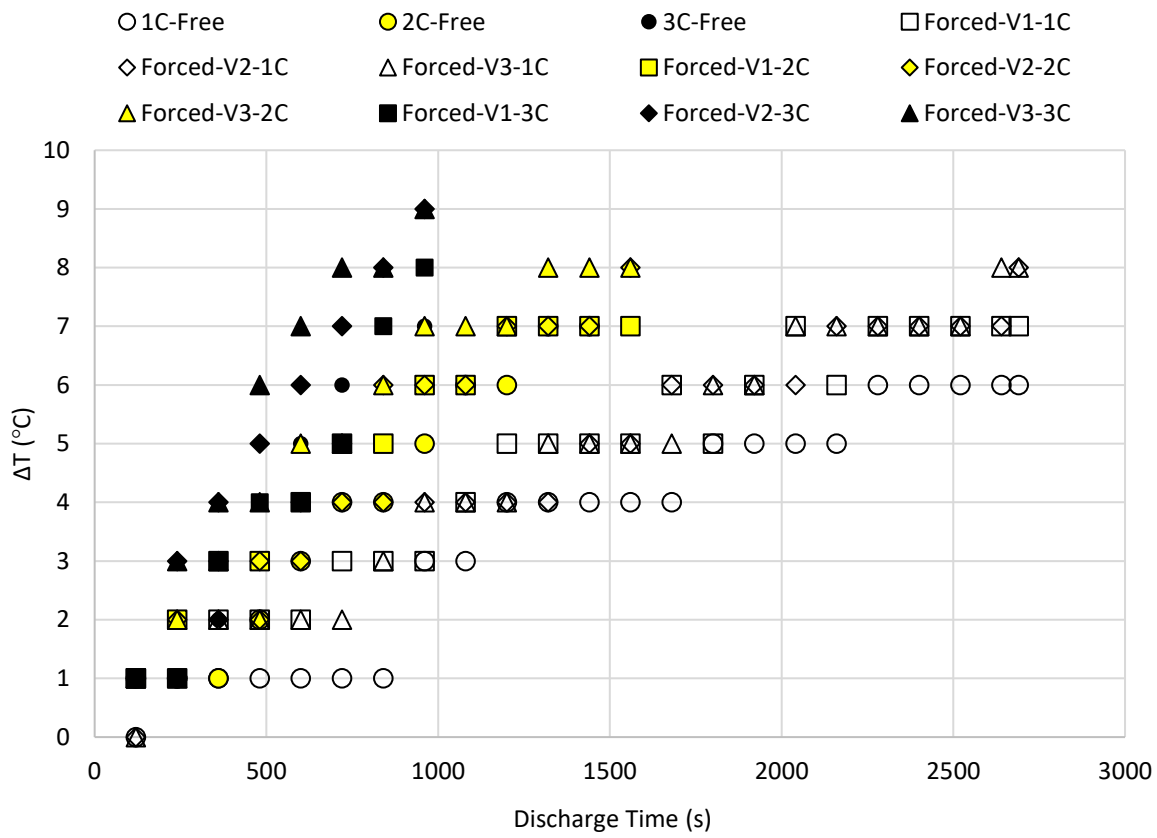

Fig. 12. Temperature homogeneity during discharge process in free and forced based BTMS at various discharge rates and inlet air velocity arrangements

3.4 Effect of Air Inlet Velocity on Performance of Forced Convection based BTMS

The forced convection cooling of battery cells is dependent on the air inlet velocity and flow pattern. To evaluate dependence of peak temperature on air inlet velocity is challenge as various variables must be considered. For present case of rectangular battery pack, results can be seen in Figure 13. Three different air velocities are selected in present study as indicate in Table 2. When velocity is increased from 3.6 m/sec to 4.6 m/sec i.e., 27% increase, there is only about 1%, 2% and 1% reduction in peak temperature respectively at 1C, 2C and 3C discharge rates. Increase air inlet velocity from 4.6 m/sec to 5.5 m/sec i.e., 20% increase, brought only 2% improvement in peak temperature at 1C, 2C and 3C rates. Although increase in air inlet velocity reduces average temperature of battery pack but it not much effective in reducing peak temperature inside battery pack. Increase in inlet air velocity has adverse effect on temperature homogeneity of battery pack as the last row cells are not cooled as efficiently as first row cells when air velocity is increased. The results of temperature homogeneity are shown in Figure 14. The results indicated that a trade-off between peak temperature and temperature homogeneity is required in forced convection and optimum air inlet velocity selection should be selected such that both these parameters remain within acceptable range of working conditions.

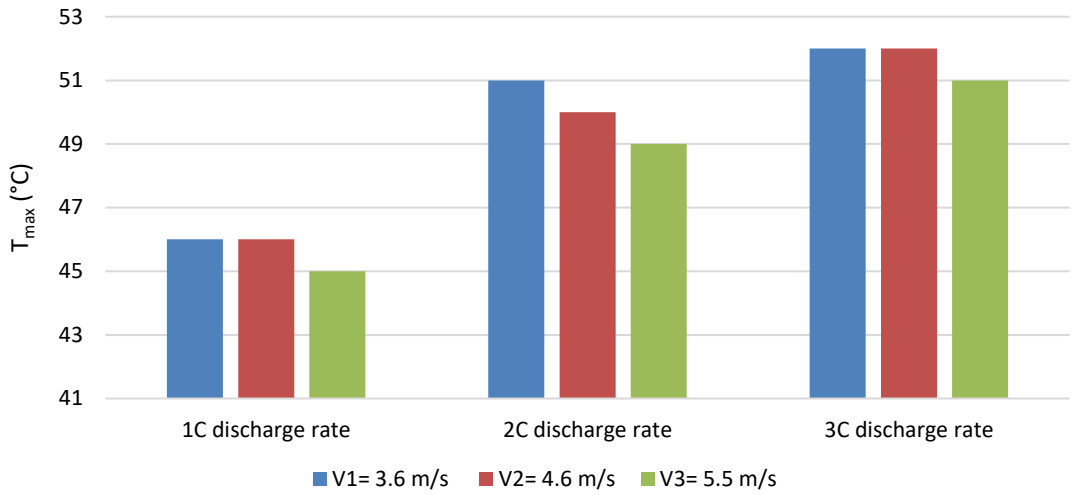

Fig. 13. Effect of change inlet air velocity on peak temperature for forced convection based BTMS at 1C, 2C and 3C discharge rates

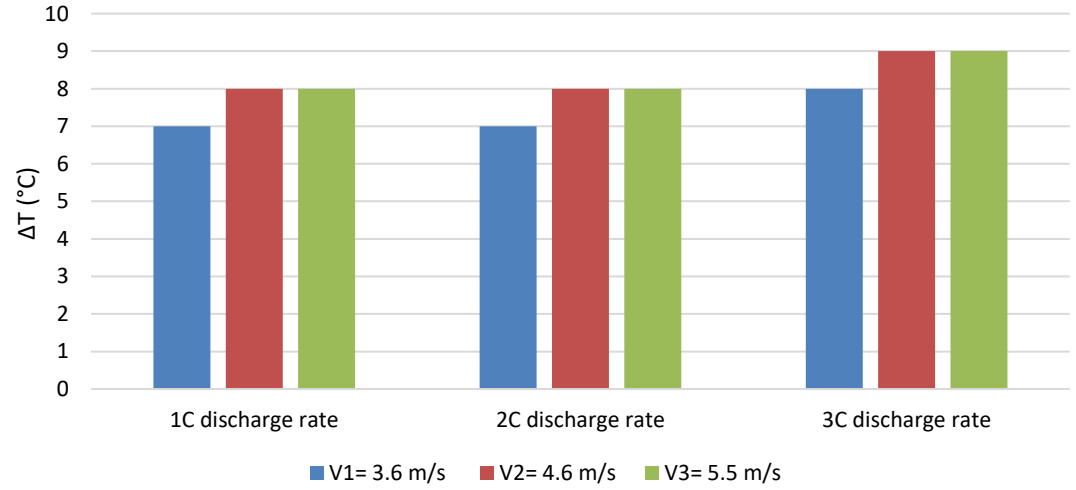

Fig. 14. Effect of change inlet air velocity on peak temperature for forced convection based BTMS at 1C, 2C and 3C discharge rates

4. Conclusions

In the present study, experimental investigations were conducted to find critical cells inside battery pack of cylindrical cells under free and forced convection. Temperature homogeneity, peak temperature and average temperature were measured while discharging battery pack at three discharge rates: 1C, 2C and 3C. Results are summarized in Table 3 and following conclusions can be drawn:

i. Both free (BTMS-FR) and forced (BTMS-FO) convection based BTMS are not able to control temperature uniformity within ideal limit of 5˚C.
ii. Centre cells (6, 7) are critical in free convection while the cells in the last row (9, 10, 11 and 12) are critical in forced convection.
iii. Row-wise temperature homogeneity of free convection is better as compared to forced convection.
iv. Free convection performs better in terms of temperature homogeneity but forced convection based BTMS performs better in terms of peak temperature and average temperature of battery pack.

v. Increasing air inlet velocity in forced convection is not significant in maintaining peak temperature and temperature homogeneity within acceptable limits, although average temperature of battery pack reduces when air inlet velocity is increased.

Table 3
BTMS-FR and BTMS-FO w.r.t threshold limits of peak temperature and temperature homogeneity

	(A) Peak temperature threshold limits			(B) Temperature homogeneity threshold limits		BTMS performance (A) ∩ (B)	
BTMS type	Ideal limit (T ≤ 40°C)	Acceptable limit (T ≤ 50°C)	Safety limit (T ≤ 60°C)	Ideal limit (ΔT ≤ 5°C)	Acceptable limit (ΔT ≤ 8°C)	Ideal	Acceptable
Free- 1C	×	×	✓	×	✓	×	×
Free- 2C	×	×	✓	×	✓	×	×
Free- 3C	×	×	✓	×	✓	×	×
Forced-V1-1C	×	✓	✓	×	✓	×	✓
Forced-V2-1C	×	✓	✓	×	✓	×	✓
Forced-V3-1C	×	✓	✓	×	✓	×	✓
Forced-V1-2C	×	×	✓	×	✓	×	×
Forced-V2-2C	×	✓	✓	×	✓	×	✓
Forced-V3-2C	×	✓	✓	×	✓	×	✓
Forced-V1-3C	×	×	✓	×	✓	×	×
Forced-V2-3C	×	✓	✓	×	×	×	×
Forced-V3-3C	×	✓	✓	×	×	×	×

References

[1] Ahmad, Zishan, Mohammad Junaid Khan, and Md Naqui Akhtar. "A Critical Review of Hybrid Electric Vehicles." *Journal of Advanced Research in Applied Sciences and Engineering Technology* 29, no. 1 (2022): 283-294. https://doi.org/10.37934/araset.29.1.283294

[2] Wang, Tao, K. J. Tseng, Jiyun Zhao, and Zhongbao Wei. "Thermal investigation of lithium-ion battery module with different cell arrangement structures and forced air-cooling strategies." *Applied Energy* 134 (2014): 229-238. https://doi.org/10.1016/j.apenergy.2014.08.013

[3] Kromer, Matthew A., and John B. Heywood. "Electric Powertrains: Opportunities and Challenges in the US Light-Duty Vehicle Fleet." *Laboratory for Energy and the Environment, Massachusetts Institute of Technology* (2007).

[4] Broussely, M., J. P. Planchat, G. Rigobert, D. Virey, and G. Sarre. "Lithium-ion batteries for electric vehicles: performances of 100 Ah cells." *Journal of Power Sources* 68, no. 1 (1997): 8-12. https://doi.org/10.1016/S0378-7753(96)02544-X

[5] Mastali, Mehrdad, Evan Foreman, Ali Modjtahedi, Ehsan Samadani, Amir Amirfazli, Siamak Farhad, Roydon A. Fraser, and Michael Fowler. "Electrochemical-thermal modeling and experimental validation of commercial graphite/$LiFePO_4$ pouch lithium-ion batteries." *International Journal of Thermal Sciences* 129 (2018): 218-230. https://doi.org/10.1016/j.ijthermalsci.2018.03.004

[6] Waldmann, Thomas, Rares-George Scurtu, Karsten Richter, and Margret Wohlfahrt-Mehrens. "18650 vs. 21700 Li-ion cells-A direct comparison of electrochemical, thermal, and geometrical properties." *Journal of Power Sources* 472 (2020): 228614. https://doi.org/10.1016/j.jpowsour.2020.228614

[7] Zhao, Rui, Sijie Zhang, Jie Liu, and Junjie Gu. "A review of thermal performance improving methods of lithium ion battery: Electrode modification and thermal management system." *Journal of Power Sources* 299 (2015): 557-577. https://doi.org/10.1016/j.jpowsour.2015.09.001

[8] Bernagozzi, Marco, Anastasios Georgoulas, Nicolas Miche, and Marco Marengo. "Heat pipes in battery thermal management systems for electric vehicles: A critical review." *Applied Thermal Engineering* 219 (2023): 119495. https://doi.org/10.1016/j.applthermaleng.2022.119495

[9] Ramadass, P., Bala Haran, Ralph White, and Branko N. Popov. "Capacity fade of Sony 18650 cells cycled at elevated temperatures: Part II. Capacity fade analysis." *Journal of Power Sources* 112, no. 2 (2002): 614-620. https://doi.org/10.1016/S0378-7753(02)00473-1

[10] Terada, N., T. Yanagi, S. Arai, M. Yoshikawa, K. Ohta, N. Nakajima, A. Yanai, and N. Arai. "Development of lithium batteries for energy storage and EV applications." *Journal of Power Sources* 100, no. 1-2 (2001): 80-92.

https://doi.org/10.1016/S0378-7753(01)00885-0
[11] Fathabadi, Hassan. "High thermal performance lithium-ion battery pack including hybrid active-passive thermal management system for using in hybrid/electric vehicles." *Energy* 70 (2014): 529-538. https://doi.org/10.1016/j.energy.2014.04.046
[12] Motloch, Chester G., Jon P. Christophersen, Jeffrey R. Belt, Randy B. Wright, Gary L. Hunt, Raymond A. Sutula, Tien Duong, Thomas J. Tartamella, Harold J. Haskins, and Ted J. Miller. *High-Power Battery Testing Procedures and Analytical Methodologies for HEV's*. No. 2002-01-1950. 2000. https://doi.org/10.4271/2002-01-1950
[13] Giuliano, Michael R., Ajay K. Prasad, and Suresh G. Advani. "Experimental study of an air-cooled thermal management system for high capacity lithium-titanate batteries." *Journal of Power Sources* 216 (2012): 345-352. https://doi.org/10.1016/j.jpowsour.2012.05.074
[14] Nagasubramanian, Ganesan. "Electrical characteristics of 18650 Li-ion cells at low temperatures." *Journal of Applied Electrochemistry* 31 (2001): 99-104. https://doi.org/10.1023/A:1004113825283
[15] Panchal, Satyam, Rocky Khasow, Ibrahim Dincer, Martin Agelin-Chaab, Roydon Fraser, and Michael Fowler. "Thermal design and simulation of mini-channel cold plate for water cooled large sized prismatic lithium-ion battery." *Applied Thermal Engineering* 122 (2017): 80-90. https://doi.org/10.1016/j.applthermaleng.2017.05.010
[16] Huang, Yuqi, Pan Mei, Yiji Lu, Rui Huang, Xiaoli Yu, Zhuolie Chen, and Anthony Paul Roskilly. "A novel approach for Lithium-ion battery thermal management with streamline shape mini channel cooling plates." *Applied Thermal Engineering* 157 (2019): 113623. https://doi.org/10.1016/j.applthermaleng.2019.04.033
[17] Yan, Jiajia, Qingsong Wang, Ke Li, and Jinhua Sun. "Numerical study on the thermal performance of a composite board in battery thermal management system." *Applied Thermal Engineering* 106 (2016): 131-140. https://doi.org/10.1016/j.applthermaleng.2016.05.187
[18] Zhang, Zhenying, Jiayu Wang, Xu Feng, Li Chang, Yanhua Chen, and Xingguo Wang. "The solutions to electric vehicle air conditioning systems: A review." *Renewable and Sustainable Energy Reviews* 91 (2018): 443-463. https://doi.org/10.1016/j.rser.2018.04.005
[19] Qin, Peng, Mengran Liao, Danfeng Zhang, Yujun Liu, Jinhua Sun, and Qingsong Wang. "Experimental and numerical study on a novel hybrid battery thermal management system integrated forced-air convection and phase change material." *Energy Conversion and Management* 195 (2019): 1371-1381. https://doi.org/10.1016/j.enconman.2019.05.084
[20] Lin, Jiayuan, Xinhua Liu, Shen Li, Cheng Zhang, and Shichun Yang. "A review on recent progress, challenges and perspective of battery thermal management system." *International Journal of Heat and Mass Transfer* 167 (2021): 120834. https://doi.org/10.1016/j.ijheatmasstransfer.2020.120834
[21] Cen, Jiwen, Zhibin Li, and Fangming Jiang. "Experimental investigation on using the electric vehicle air conditioning system for lithium-ion battery thermal management." *Energy for Sustainable Development* 45 (2018): 88-95. https://doi.org/10.1016/j.esd.2018.05.005
[22] Basri, Mahamad Hisyam Mahamad, Yusli Yaakob, Zulkhairi Kamaruzaman, Fairosidi Idrus, Norasikin Hussin, and Idris Saad. "Heat Pipe as a Passive Cooling Device for PV Panel Performance Enhancement." *Journal of Advanced Research in Applied Sciences and Engineering Technology* 28, no. 2 (2022): 190-198. https://doi.org/10.37934/araset.28.2.190198
[23] Behi, Hamidreza, Danial Karimi, Mohammadreza Behi, Joris Jaguemont, Morteza Ghanbarpour, Masud Behnia, Maitane Berecibar, and Joeri Van Mierlo. "Thermal management analysis using heat pipe in the high current discharging of lithium-ion battery in electric vehicles." *Journal of Energy Storage* 32 (2020): 101893. https://doi.org/10.1016/j.est.2020.101893
[24] Singh, Manmeet, and Ravindra Jilte. "Development of experimental facility for testing battery thermal management system of electrical vehicles." *Materials Today: Proceedings* 72 (2023): 1917-1924. https://doi.org/10.1016/j.matpr.2022.10.154
[25] Žukauskas, Algirdas. "Heat transfer from tubes in crossflow." In *Advances in Heat Transfer*, vol. 8, pp. 93-160. Elsevier, 1972. https://doi.org/10.1016/S0065-2717(08)70038-8
[26] Churchill, Stuart W., and Humbert H. S. Chu. "Correlating equations for laminar and turbulent free convection from a vertical plate." *International Journal of Heat and Mass Transfer* 18, no. 11 (1975): 1323-1329. https://doi.org/10.1016/0017-9310(75)90243-4
[27] Kosky, Philip, Robert Balmer, William Keat, and George Wise. "Chapter 12 - Mechanical Engineering." In *Exploring Engineering (Third Edition)*, pp. 259-281. Academic Press, 2013. https://doi.org/10.1016/B978-0-12-415891-7.00012-1